



OPEN Influence of rock heterogeneity on the correlation between uniaxial compressive strength and Brazilian tensile strength

Fanmeng M. Kong^{1,2✉}, Mingyi Han², Yuting T. Zhao^{1,3✉}, Haitao Lu³, Shian Liu^{1,3}, Pengyu Luan^{1,3}, Baolong Zhuo⁴ & Gaofei Shi^{1,3}

To offer guidance for using Brazilian tensile strength (BTS) to estimate UCS of heterogeneous rocks, this study uses sandstone (fine or coarse grain) and gneiss (0°, 45°, 90° inclined anisotropy) to investigate the influence of grain size or anisotropy on the correlations of UCS-BTS. According to the regression analysis, there is no significant equation of UCS-BTS for rocks with vertical anisotropy. The grain size variation or multidirectional anisotropy can result in a decrease in the determination coefficient value of correlations. Then, coarse grain size or vertical anisotropy deteriorates the statistical performance of correlations between UCS and BTS, reflected by the Akaike Information Criterion and performance index. For rocks with fine grain size or 45° inclined anisotropy, the data points of estimated UCS are clustered uniformly around the exact estimation line. Finally, the accuracy of predicted UCS via BTS declines obviously following the varying grain size or different anisotropy orientations. Using empirical formulas with different grain sizes or anisotropy properties can generate significant errors in estimated UCS. To predict UCS, BTS should be extracted from rocks with single grain size magnitude or unidirectional anisotropy. Moreover, the Brazilian test parallel to the anisotropy cannot be used to derive the correlation of UCS-BTS.

Keywords Grain size, Anisotropy, Correlation, Uniaxial compressive strength, Brazilian tensile strength

Uniaxial compressive strength (UCS) has been widely referenced by the rock mass classification systems (i.e., RMR (rock mass rating)¹ or rock failure criteria (i.e., Hoek-Brown criterion)^{2,3}, which acted as the reliable basis for the design of underground structures and slope stabilization^{4–6}. Also, UCS is an extremely significant mechanical parameter for civil and infrastructure projects, such as dams and foundations^{7–10}.

The standard testing methods of UCS have been suggested by the ISRM (International Society for Rock Mechanics)¹¹ and ASTM (American Society for Testing and Materials)¹². However, the laboratory experiments of UCS require standard core specimens whose drilling procedure is time-consuming and expensive, especially for the extremely hard, soft, highly fractured or thinly bedding rocks^{13–16}. Thus, the indirect methods for estimating UCS have been considered by many academics and practitioners^{17–19}. According to the Griffith's theory of failure, the UCS was eight times the tensile strength of rock. As such, numerous papers attempted to derive the correlations between UCS and Brazilian tensile strength (BTS) since the 1950s.

The pioneering study on this topic was presented by Hosking²⁰ and the conversion factors between UCS and BTS fluctuated from 4 to 10. Then, increased attention was directed toward coal or coal measure rocks^{21,22}. Apart from the zero-intercept linear equation, intercept linear function was also proposed for the correlations of UCS-BTS^{23,24}.

Weathering is a crucial factor in deteriorating the mechanical properties of rock, and the conversion factors of UCS-BTS were different for the fresh and decomposed rocks. For example, Lumb²⁵ found that the ratio of UCS to BTS was 14 for fresh rock and 8 for weathered rock, respectively. This study was followed by Gupta and Rao²⁶, where the conversion factor between UCS and BTS ranged due to the weathered degree of rock.

¹Key Laboratory of Geological Safety of Coastal Urban Underground Space, MNR, Qingdao 266101, China. ²School of Engineering and Technology, China University of Geosciences (Beijing), Beijing 100083, China. ³Qingdao Geo-Engineering Surveying Institute (Qingdao Geological Exploration Development Bureau), Qingdao 266101, China. ⁴Qingdao Geological and Mineral Geotechnical Engineering Co, Ltd, Qingdao 266101, China. ✉email: kongfanmeng10@cugb.edu.cn; zhao_yuting@126.com

In 2010, Altindag and Guney²⁷ first derived a power correlation of UCS-BTS. After that, three function types, linear, power, and exponential, were presented for the equations of estimating UCS through BTS of rock from various geological origins (see Table 1). Recently, Kong et al. (2024) collected the UCS and BTS data from worldwide studies since the 1950s and found that UCS is nearly eight times BTS. This finding can support Griffith's theory of failure.

Moreover, it was found that the correlations of UCS-BTS were significantly affected by the rock heterogeneity, such as grain size variation and weak planes (i.e., anisotropy including geological bedding, schistosity, foliation or gneissosity)^{50,51}. Coarse-grained rock has a higher value of BTS, where the coarser quartz acts as the main stress-bearing skeleton⁵². Besides, coarse grains result in an increased discreteness degree of BTS data, reflected by the higher values of coefficient of variation⁵³.

Meanwhile, it was noted that BTS increased as the anisotropy angle increased from 0° to 90°^{54,55}. The maximum BTS can be obtained from the rock specimen with horizontal anisotropy, while the smallest value is observed at different anisotropy angles for different rocks^{56,57}. Also, the discreteness of BTS data decreases continuously following the increasing anisotropy inclination⁵³.

Based on the above review, the impacts of grain size or anisotropy on the Brazilian test have been widely explored; but, how the correlation of UCS-BTS responds to lithological heterogeneities remains unexplained. And yet, isotropic and homogeneous rocks are seldom found in nature. To direct using Brazilian test to predict UCS of heterogeneous rock, this study will investigate the effects of grain size or anisotropy on the correlations between UCS and BTS. Then, the deviations of estimated UCS derived from rock heterogeneity can be minimized. The results of this work can potentially improve the accuracy of estimated UCS, which is essential for rock engineering.

To achieve this goal, this study will perform UCS and Brazilian tests on two typical heterogeneous rocks, i.e., sandstones with different grain sizes and gneiss with visible gneissosity. This was followed by the regression analysis used to derive the correlation of UCS-BTS. Then, the influence of grain size or anisotropy on the

Equations	R ²	Rock-types	No. of samples	References
UCS=(4-10)BTS	–	–	–	Hosking ²⁰
UCS=(17-28)BTS	–	Coal	–	Pomeroy and Foote ²¹
UCS=3.27BTS – 0.97	–	Limestone, sandstone, mudstone and siltstone	–	Hobbs ²³
UCS=2.84BTS – 3.39	–	Limestone, sandstone, mudstone and siltstone	–	Hobbs ²⁴
UCS=3.6BTS+15.2	–	Coal measure rocks	229	Szlavin ²²
UCS=(8-14)BTS	–	Igneous rocks (Hong Kong, China)	–	Lumb ²⁵
UCS=(7.9-9.72)BTS	–	Granite, basalt, quartzite (India)	13	Gupta and Rao ²⁶
UCS=12.2BTS	–	Limestone (Nigeria)	–	Teme ²⁸
UCS=(10-20)BTS	–	Mudstone, limestone, granite, sandstone	–	Brook ²⁹
UCS=(5-50)BTS	–	Various rock types	–	Lade ³⁰
UCS=6.71BTS+36.0	0.61	Sandstone (South Africa)	27	Bell and Lindsay ³¹
UCS=(6.74-10.26)BTS	–	Granite and limestone	–	Din and Rafiq ³²
UCS=6.67BTS+0.73	0.92	Granite, granodiorite (Turkey)	10	Tuğrul and Zarfı ³³
UCS=8BTS	–	Brittle rocks	–	Brady and Brown ³⁴
UCS=6.8BTS+13.5	0.65	Greywackes (Turkey)	82	Gokceoglu and Zorlu ³⁵
UCS=4.9BTS	–	Calcarene	5	Coviello et al. ³⁶
UCS=6.2BTS	–	Gasbeton	–	
UCS=2.38BTS ^{1.0725}	0.79	Limestone, granite, marble (Turkey)	–	Altindag and Guney ²⁷
UCS=2.86e ^{0.015} BTS	–	Coal	–	Arioglu and Tokgoz ³⁷
UCS=10.61BTS	0.54	Limestone, marble, Serpentine (Turkey)	46	Kahraman et al. ³⁸
UCS=5.86BTS+17.5	–	Limestone (Iran)	32	Rajabzadeh et al. ³⁹
UCS=8.60BTS – 27.57	–	Diagenetic dolomitic limestone (Iran)	–	Sivakugan et al. ⁴⁰
UCS=12.4BTS – 9.0	–	–	–	
UCS=7.22BTS+40.077	0.61	Granite, granodiorite (Turkey)	6	Yesiloglu-Gultekin et al. ⁴¹
UCS=4.874BTS+24.301	0.90	Metabasalt, dacite, basalt (Turkey)	37	Karaman et al. ⁴²
UCS=15.36BTS – 10.303	–	Shale, old alluvium (Nusajaya, Malaysia)	40	Mohamad et al. ⁴³
UCS=10.03BTS+55.19	0.92	Hornfels schist (Iran)	8	Fereidooni ⁴⁴
UCS=10.4BTS+18.2	0.63	Flint (Europe)	7	Aliyu et al. ¹³
UCS=3.469BTS+15.73	–	Travertine (Iran)	32	Ebdali et al. ⁴⁵
UCS=7.73BTS ^{1.197}	0.90	Andesite, limestone, marble (Turkey)	93	Teymen and Mengüç ⁴⁶
UCS=4.2327BTS+13.638	0.53	Gypsum (United Arab Emirates)	48	Arman ⁴⁷
UCS=7.26BTS	0.95	Carbonate rocks (Iran)	107	Sadeghi et al. ⁴⁸
UCS=8.1442BTS	0.83	Various	443	Kong et al. ⁴⁹

Table 1. The representative correlations between UCS (MPa) and Brazilian tensile strength (MPa).

correlation between UCS and BTS will be explored in three aspects: (1) the discreteness of uniaxial compressive and Brazilian testing data; (2) variation of the parameters of regression analysis (3) discrepancies between measured UCS and estimated UCS via BTS. Finally, a comparison study was performed by comparing the proposed equations with the previous studies.

Sample preparation and laboratory experiments

To eliminate the lithological effect, sandstones with different grain size magnitudes, i.e., fine (<0.1 mm) and coarse grain (>0.25 mm), were sampled from the identical geological cross-section in Zibo City, China. Also, gneiss blocks (with visible gneissosity) were collected from Neo-archean intrusive rocks in Jining City, China. The heterogeneous characteristics of rock samples were observed through the thin section photomicrographs (see Fig. 1). It was noted that grain size variation and anisotropy (i.e., non-persistent gneissosity) were displayed clearly under the microscale. For the UCS and Brazilian tests, the drilling sampler with a diameter of 50 mm was used to obtain the standard cylindrical specimens. To obtain gneiss samples with different anisotropy inclinations, rock blocks were drilled normal, at 45°, or parallel to the gneissosity (Fig. 2). A total of 14 sandstone samples and 19 gneiss samples were prepared for the following laboratory experiments.

The uniaxial compressive tests were conducted based on the recommendation of China national standard⁵⁸. Core samples have a diameter of 50 mm and a height of 100 mm, respectively (Fig. 3). The standard cylindrical specimens were uniaxially compressed with a loading rate of 0.5 MPa/s. The final UCS is the mean result of three specimens (Tables 2 and 3).

The same machine, possessing the ability to exert and measure axial load on rock specimens (with a loading rate of 0.5 MPa/s), was utilized for the Brazilian test. To produce uniform tensile stress distribution, two steel loading jaws were used to contact the disc-shaped rock specimen at diametrically opposed surfaces (Fig. 3). Rock specimens have a diameter of 50 mm and a height-to-diameter ratio of 0.5. The test should be repeated 3 times for each sample type (Tables 2 and 3), and the Brazilian tensile strength-BTS (MPa) can be determined as the following Eq.

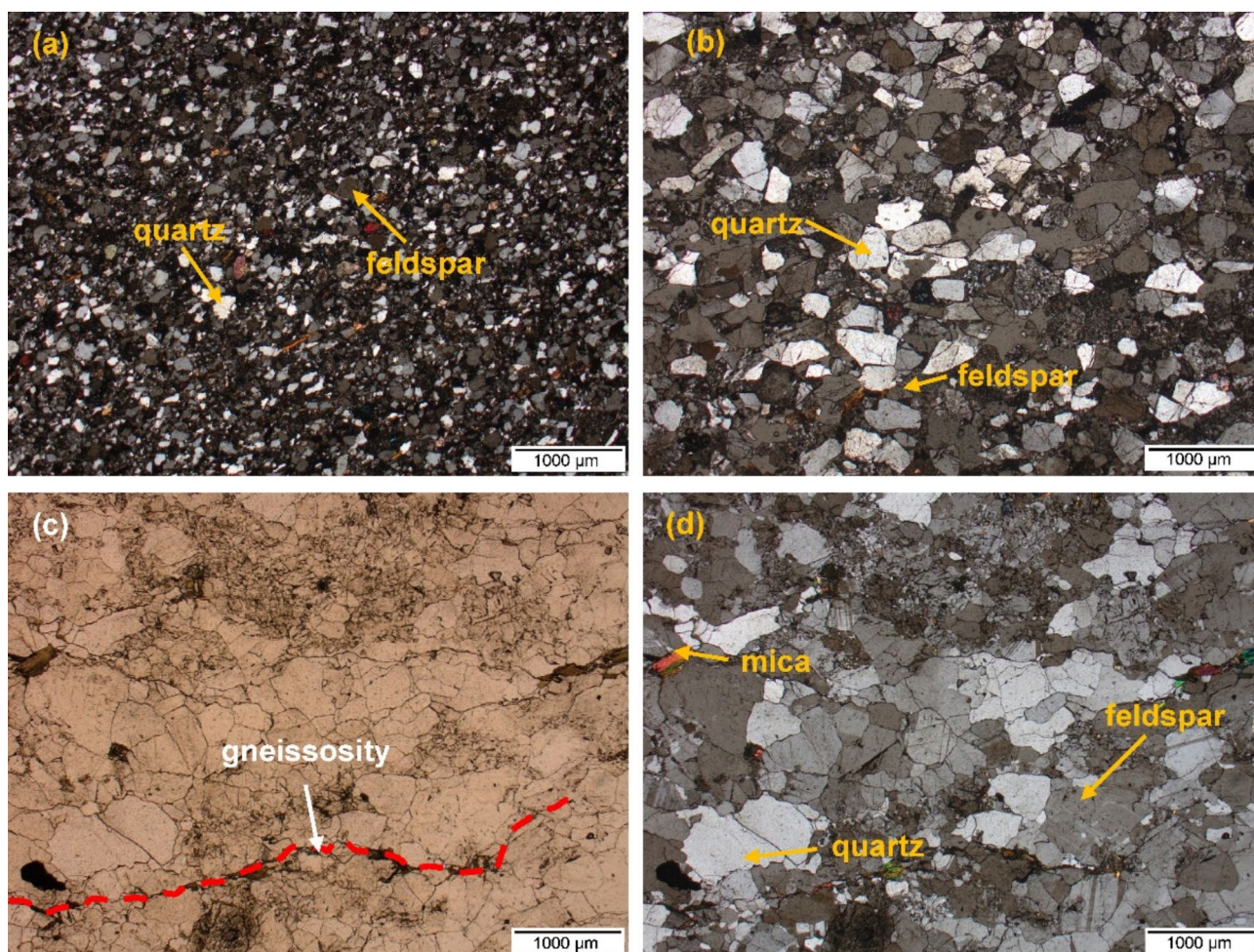


Fig. 1. Thin section photomicrographs of rock specimens. (a) Fine-grained sandstone; (b) coarse-grained sandstone; (c) gneiss observed under plane-polarized light; (d) gneiss presented under cross-polarized light.

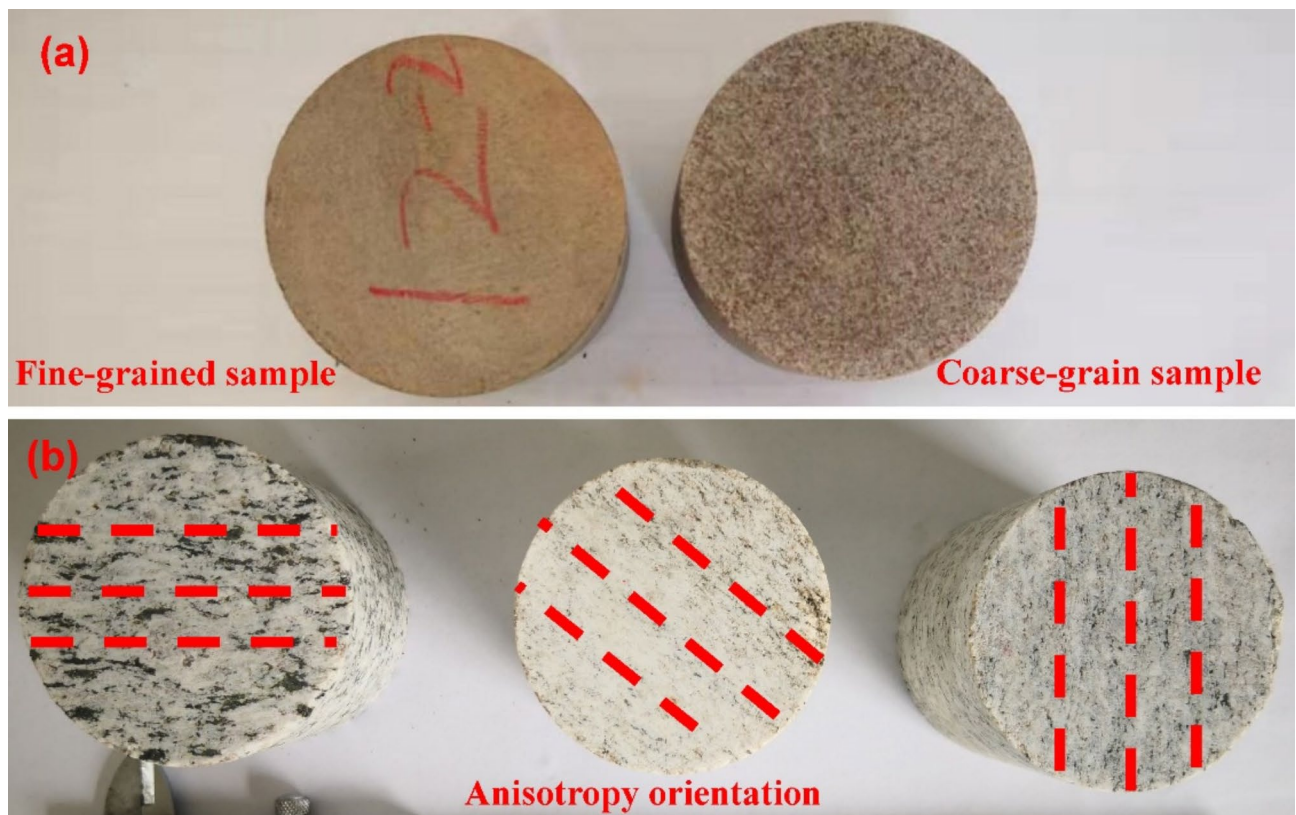


Fig. 2. The characterization of rock samples used in this study. (a) Sandstone samples with different grain size; (b) gneiss samples with different gneissosity orientations.

$$BTS = \frac{2P}{\pi Dt} \quad (1)$$

where P is the peak load at failure (N); D and t is the diameter and thickness of rock specimens (mm), respectively.

Regression analysis

In this study, regression analysis will be used to derive the correlations between UCS and BTS. Four function types including linear, power, exponential and logarithmic are evaluated for the correlation and the equation with the highest determination coefficient (R^2) was regarded as the best-fitting function. To verify the significance of the proposed equation, parameter of P-value was calculated concerning the 95% confidence interval. Once the P-value is smaller than 0.05, there is a real correlation between UCS and BTS.

Figures 4 and 5; Table 4 show the regression analysis results and its corresponding parameters. It is noted that zero-intercept linear equations of UC-BTS are presented for almost all the sample types, apart from rocks with vertical anisotropy. Also, the magnitudes of the P-value of the above formulas are lower than the limit of 0.05, which means the correlations between UCS and BTS are significant. However, there are no real correlated equations between UCS and BTS for gneiss with $\beta = 90^\circ$, reflected by the P-value (larger than 0.05) and R^2 (0.0198). Moreover, the proposed equations give somewhat different magnitudes of R^2 value. Thus, the significance of proposed formulas fluctuates dramatically following changing grain size or anisotropy orientation.

Results interpretation, comparison and discussion

Influences of grain size or anisotropy on the parameters of regression analysis

Grain size or anisotropy is suspected to have a significant impact on the correlations between UCS and BTS, which can be demonstrated by the different parameters of regression analysis. The UCS of either fine-grained sandstone or coarse-grained sandstone shows a high correlated degree with BTS, whose R^2 value is 0.985 and 0.958, respectively. For the rock samples containing different magnitudes of grain size, the correlated degree between UCS and BTS declines significantly and has an R^2 of 0.876. Meanwhile, the R^2 value of the proposed equations decreases evidently when the grain size shifts from fine grain to coarse grain.

Consistent with the effect of grain size variation, multidirectional anisotropy results in a decline of correlated degrees between UCS and BTS, favored by the R^2 value of 0.887. Then, the UCS of rock specimens containing unidirectional anisotropy has a higher correlated degree with BTS, where R^2 values of rocks with horizontal and 45° inclined anisotropy are 0.962 and 0.988, respectively. However, there is no real correlation between UCS and BTS and the P-value of this empirical formula is larger than 0.05 (Table 4).

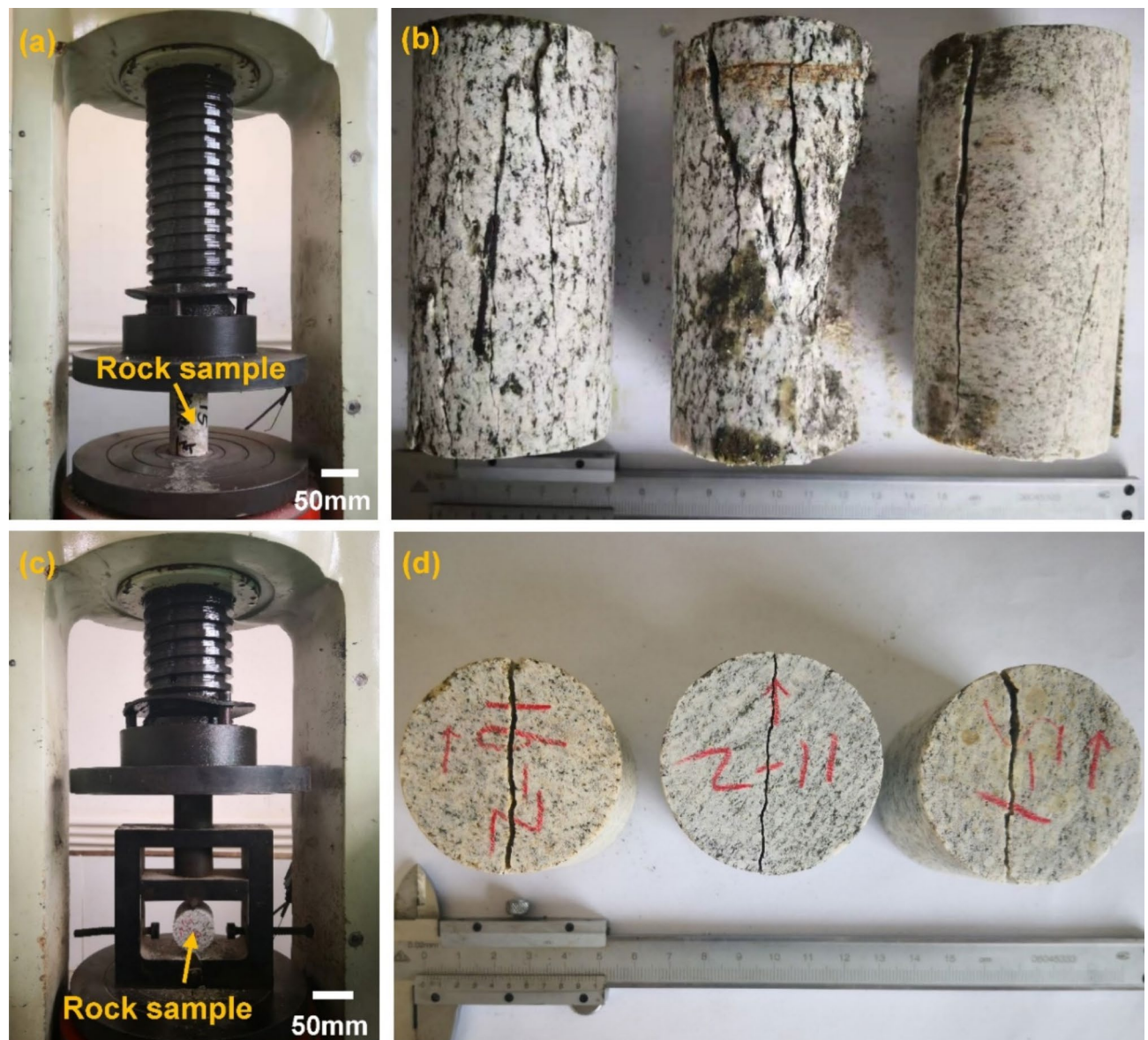


Fig. 3. Laboratory experimental setup. (a, b) Uniaxial compressive test; (c, d) Brazilian test.

Thus, coarse grain size has a significant impact on the Brazilian test in the UCS estimation, changing the conversion factor and eventually reducing the correlated degree between UCS and BTS. On the other hand, decreases in grain size are accompanied by increasing R^2 value. This is likely to be caused by different discrete degrees of UCS data. It is noted that the COVs of UCS from fine-grained sandstone change between 0.72% and 11.03% while the UCS of coarse-grained sandstones have a COV fluctuating range from 1.03 to 24.62%. The UCS of fine-grained sandstone has a relatively smaller discrete degree than the coarse-grained sandstone.

The BTS of rocks with 45° inclined anisotropy show the highest correlated degree to UCS. Also, the vertical anisotropy makes the equation of UCS-BTS insignificant. The potential causes of this phenomenon may be generated by different responses to anisotropy for the UCS and BTS test. The stress states of UCS and BTS are compressive and tensile, respectively. Previous study indicates that rock is more brittle and much easier to be fractured at 30° inclined anisotropy due to the uniaxial compressive stress⁵⁹. However, the biggest BTS is observed from the rock with horizontal anisotropy, while the smallest value is from vertical anisotropic rock⁶⁰. This means that rock prefers to fracture along the vertical anisotropy and the BTS reflects the strength of weak planes, rather than the rock strength itself. Therefore, it is impossible to derive a correlation between the strength of rock and weak plane.

Influences of grain size or anisotropy on the estimated capability of correlations between UCS and BTS

Two statistics indices including Akaike Information Criterion (AIC) and performance index (PI) will be used to evaluate the UCS estimation performance of proposed equations. The smallest AIC value and biggest PI

Sample No.	Sample description	Uniaxial compressive test UCS		Brazilian test BTS	
		Magnitude \pm STD (MPa)	COV (%)	Magnitude \pm STD (MPa)	COV (%)
A	Fine-grained sandstone	81.53 \pm 3.16	3.88	3.94 \pm 0.81	20.56
B		86.11 \pm 1.95	2.26	5.61 \pm 0.10	1.78
C		97.13 \pm 0.70	0.72	6.99 \pm 1.67	23.89
D		85.88 \pm 7.79	9.07	6.22 \pm 1.58	25.40
E		158.97 \pm 12.13	7.63	11.07 \pm 1.64	14.81
F		112.35 \pm 12.39	11.03	7.41 \pm 2.19	29.55
G		81.71 \pm 8.00	9.79	4.06 \pm 0.80	19.70
H	Coarse-grained sandstone	137.14 \pm 3.42	2.49	4.93 \pm 1.04	21.10
I		105.01 \pm 22.39	21.32	3.09 \pm 1.09	35.28
J		116.15 \pm 7.21	6.20	3.63 \pm 0.92	25.34
K		131.70 \pm 32.43	24.62	3.26 \pm 0.64	19.63
L		114.44 \pm 25.14	21.97	2.49 \pm 0.42	16.87
M		57.37 \pm 0.59	1.03	3.43 \pm 0.88	25.66
N		72.47 \pm 15.00	20.69	3.75 \pm 0.78	20.80

Table 2. Results of laboratory experiments on sandstone and corresponding STD and COV. *STD* Standard Deviation, *COV* coefficient of variation.

Sample No.	Sample description	Uniaxial compressive test UCS		Brazilian test BTS	
		Magnitude \pm STD (MPa)	COV (%)	Magnitude \pm STD (MPa)	COV (%)
A	Gneiss ($\beta = 0^\circ$)	71.20 \pm 13.16	15.65	3.98 \pm 1.66	41.71
B		126.67 \pm 8.74	6.90	4.75 \pm 0.75	15.79
C		126.68 \pm 4.92	3.88	5.47 \pm 1.41	25.78
D		100.80 \pm 7.71	7.65	5.02 \pm 1.76	35.06
E		43.39 \pm 2.11	4.86	2.56 \pm 0.37	14.45
F		73.25 \pm 3.95	5.39	4.94 \pm 0.94	19.03
G	Gneiss ($\beta = 45^\circ$)	99.07 \pm 9.04	9.12	3.74 \pm 0.65	17.38
H		59.53 \pm 5.38	9.04	2.23 \pm 0.62	27.80
I		79.58 \pm 14.95	18.79	2.45 \pm 0.31	12.65
J		106.13 \pm 6.64	6.25	3.46 \pm 0.25	7.23
K		70.31 \pm 1.37	1.93	1.91 \pm 0.03	1.57
L		82.38 \pm 22.39	27.18	3.09 \pm 0.28	9.06
M	Gneiss ($\beta = 90^\circ$)	106.08 \pm 5.78	5.45	4.03 \pm 0.43	10.67
N		99.89 \pm 4.96	4.96	1.41 \pm 0.28	19.86
O		96.93 \pm 11.14	11.49	3.43 \pm 0.19	5.54
P		121.30 \pm 6.67	5.50	1.72 \pm 0.11	6.40
Q		109.85 \pm 13.83	12.59	4.35 \pm 0.41	9.43
R		114.64 \pm 8.57	7.47	2.34 \pm 0.12	5.13
S		91.37 \pm 0.16	0.17	2.69 \pm 0.35	13.01

Table 3. Results of laboratory experiments on gneiss and corresponding STD and COV. *STD* Standard Deviation, *COV* coefficient of variation.

value represent the best UCS estimated capability of correlation between UCS and BTS. The above two statistics indices can be calculated as follows.

$$AIC = N \ln \left[\sum_{i=1}^N \frac{(y - y')^2}{N} \right] + 2n_p \quad (9)$$

where N is the sample quantities; y is actual UCS; y' is estimated UCS; n_p is the number of parameters must be estimated.

$$PI = \left[R^2 + \left(\frac{VAF}{100} \right) - RMSE \right] \quad (10)$$

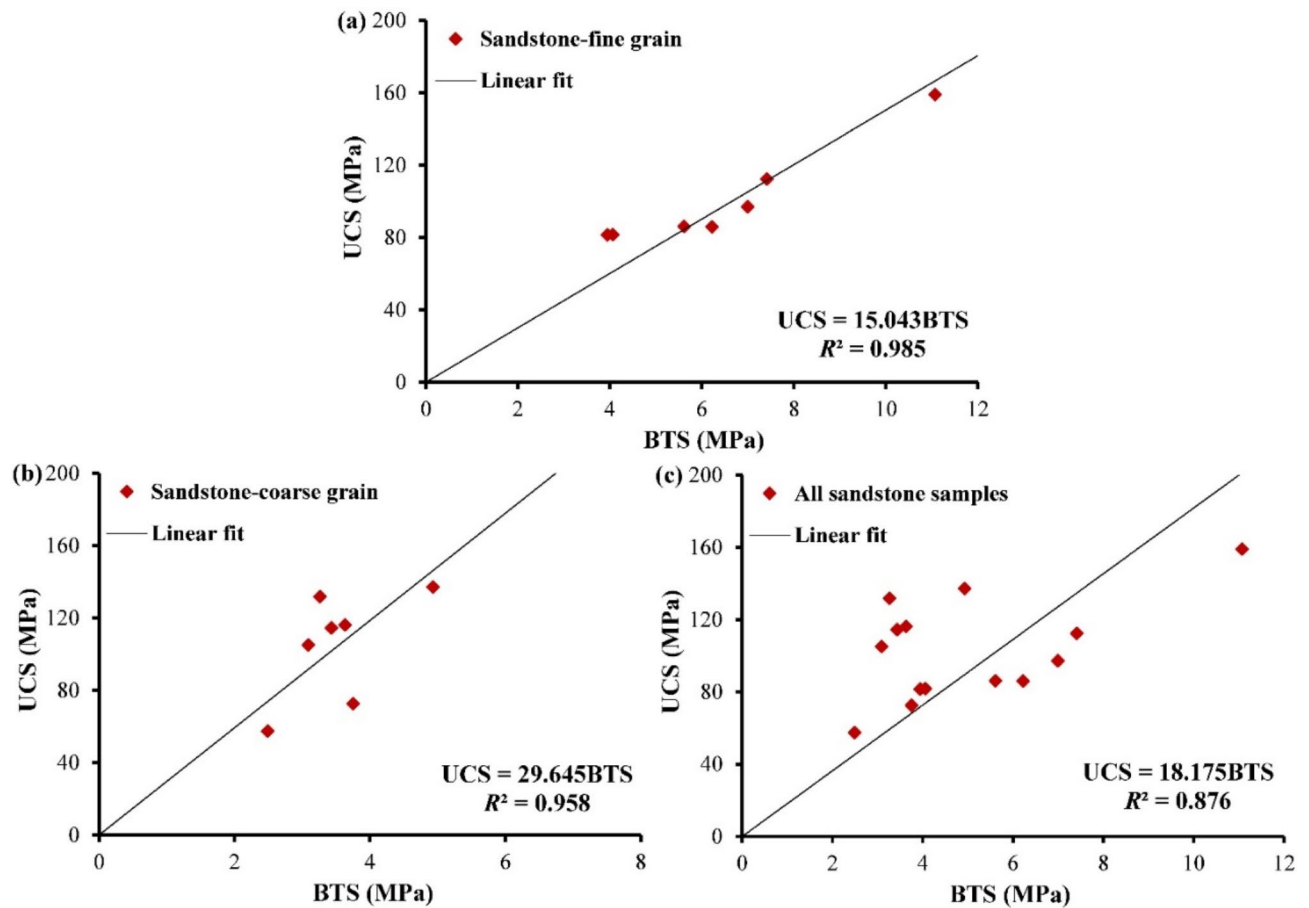


Fig. 4. Equations between UCS and BTS of sandstone. (a) Fine-grain size; (b) coarse-grain size; (c) all sandstone samples.

where R^2 is the determination coefficient; VAF is the variance accounts for (%); RMSE is the root-mean-square error.

The R^2 , VAF and RMSE can be calculated due to the following equations:

$$R^2 = 1 - \frac{\sum (y_i - y')^2}{\sum (y_i - \bar{y})^2} \quad (11)$$

$$VAF = \left[1 - \frac{\text{var}(y - y')}{\text{var}(y)} \right] \times 100 \quad (12)$$

$$RMSE = \sqrt{\frac{1}{n} \sum_{i=1}^N (y - y')^2} \quad (13)$$

where \bar{y} is the average value of actual UCS; var is variance; n is the freedom degree.

Table 4 list the AIC and PI values of derived equations. The UCS estimation capabilities of correlation between UCS and BTS weaken substantially following the growth of grain size, which can be verified by the increasing AIC value and decreasing PI value. The Brazilian test performed on rocks containing different grain size magnitudes shows the worst UCS estimated capability, and the corresponding correlation of UCS-BTS has an AIC of 103.43 and PI of -133.43, respectively.

The correlation of UCS-BTS from rock with 45° inclined anisotropy has the smallest AIC and biggest PI value, which indicates this empirical equation is most reliable in the UCS prediction. Rock samples with horizontal anisotropy show an inferior UCS estimated capability. The vertical anisotropy makes the correlation of UCS-BTS insignificant, but this phenomenon cannot be seen from the performance of AIC and PI values. Also, the UCS estimation capability of the Brazilian test is deteriorated by the multidirectional anisotropy.

Moreover, the estimated UCS via BTS were plotted against the measured UCS, and a data point located on the 1:1 diagonal line (red line in Figs. 6 and 7) indicated the exact estimation. As seen from Fig. 6, the points of estimated UCS are clustered uniformly around the diagonal lines, especially for the samples of fine-

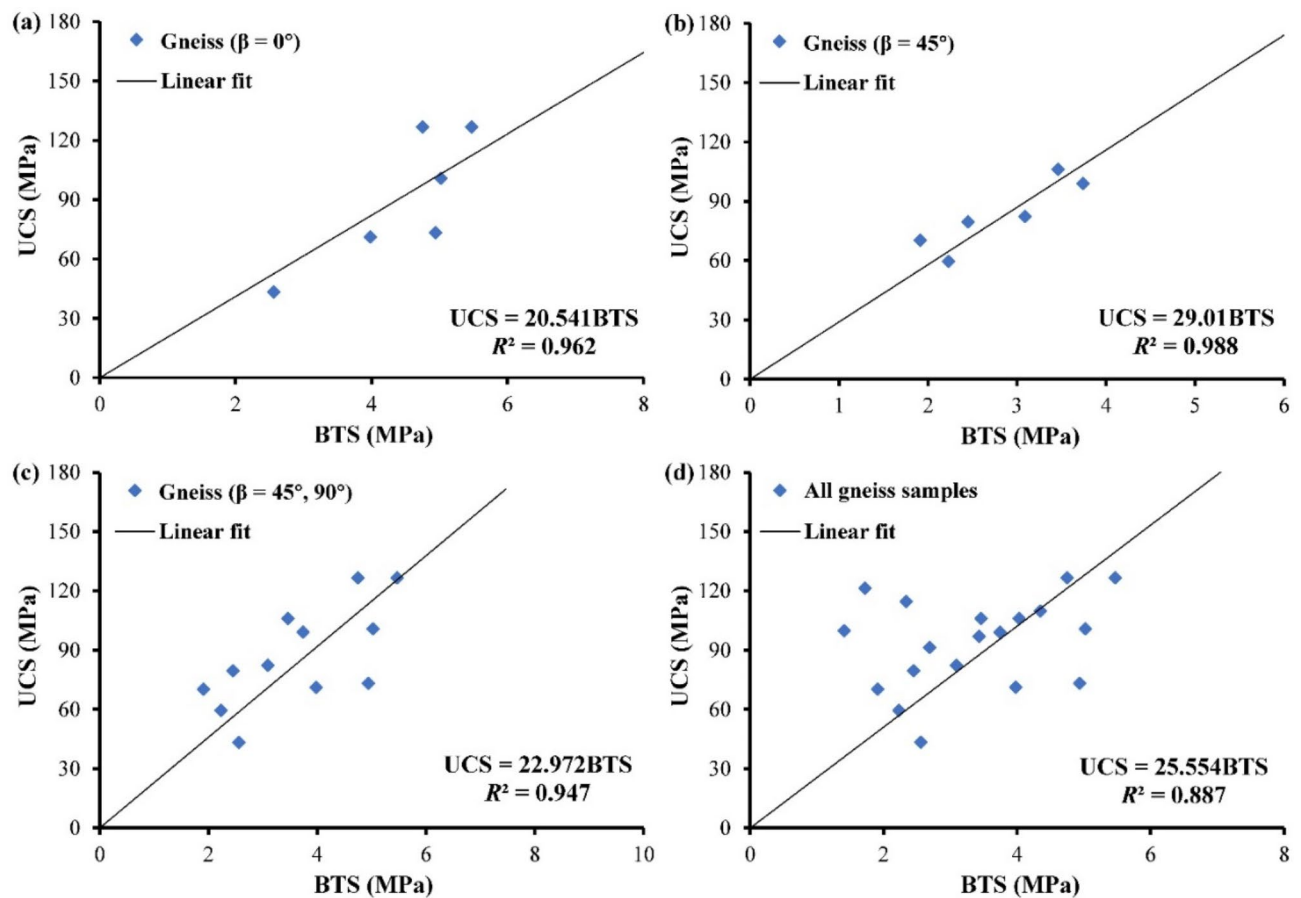


Fig. 5. Equations for correlating UCS to BTS of gneiss. (a) Samples with horizontal anisotropy; (b) samples with 45° inclined anisotropy; (c) samples with 45° and 90° inclined anisotropy; (d) all gneiss samples.

Sample types	Equation	Equation No.	R^2	P-value	AIC	PI
Fine grain size	$UCS=15.043BTS$	(1)	0.985	1.55×10^{-6}	37.44	63.86
Coarse grain size	$UCS=29.645BTS$	(2)	0.958	2.43×10^{-5}	45.49	10.52
All sandstone samples	$UCS=18.175BTS$	(3)	0.876	2.24×10^{-7}	103.43	-133.43
Gneissosity: $\beta = 0^\circ$	$UCS=20.541BTS$	(4)	0.962	9.42×10^{-5}	37.00	44.03
Gneissosity: $\beta = 45^\circ$	$UCS=29.01BTS$	(5)	0.988	4.96×10^{-6}	28.49	59.70
Gneissosity: $\beta = 90^\circ$	$UCS=-1.306BTS+109.45$	(6)	0.0198	0.76	33.65	-8.35
Gneissosity: $\beta = 45^\circ, 90^\circ$	$UCS=22.972BTS$	(7)	0.947	2.21×10^{-8}	74.65	15.91
All gneiss samples	$UCS=25.554BTS$	(8)	0.887	6.00×10^{-10}	134.18	-141.93

Table 4. The results of the regression analysis.

grained sandstone. The distances between data points and diagonal line increase evidently due to the coarse grain size. Once the rock samples contain different grain size magnitudes, the data points will deviate further compared with fine or coarse grain size. Similarly, for the rock samples containing unidirectional anisotropy, a slightly smaller discrepancy was observed between the estimated UCS and measured UCS. Different anisotropy orientations lead to an escalation of the discrepancies of estimated UCS and the data points are scattered around the diagonal line (see Fig. 7).

Moreover, the relative errors (RE) and mean absolute percentage error (MAPE) of estimated UCS are used to ulteriorly illuminate the effects of grain size or anisotropy on estimated UCS through BTS, and the above two parameters can be calculated based on the following formulas:

$$RE = \left(\frac{y - y'}{y} \right) \times 100 \quad (14)$$

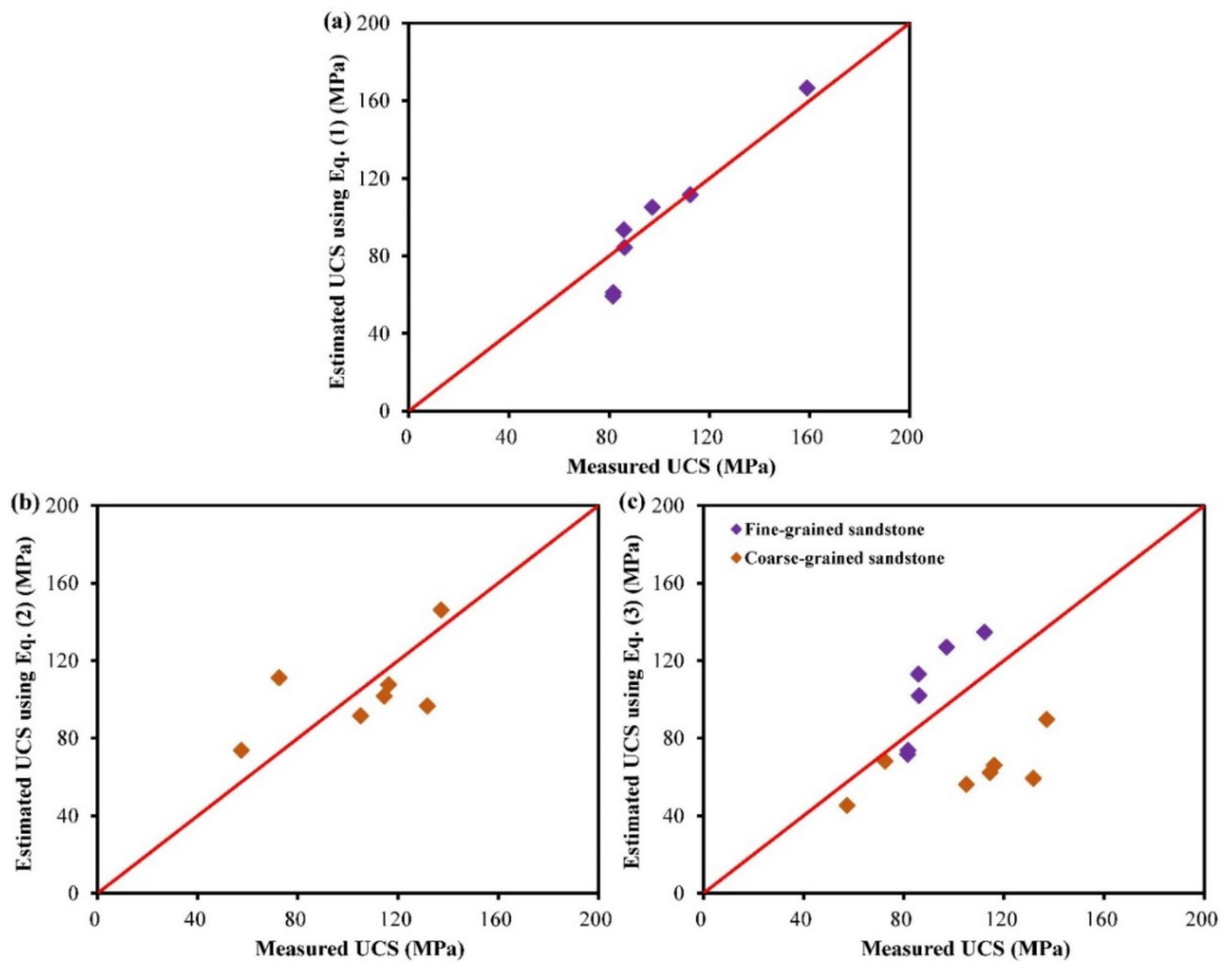


Fig. 6. Estimated capabilities of the derived equations of sandstone. (a) Fine-grain size; (b) coarse-grain size; (c) all sandstone samples.

$$\text{MAPE} = \frac{1}{N} \sum_{i=1}^N \left| \frac{(y - y')}{y} \right| \times 100 \quad (15)$$

The RE and MAPE values of estimated UCS are listed in Tables 5 and 6, and changing rules of RE for each estimated UCS data are also shown in Figs. 8 and 9. As seen in Fig. 8, the RE values of estimated UCS from rocks with grain size magnitudes have a wide fluctuating range, changing between -55.01% and 31.63% . Meanwhile, the MAPE value reaches up to 28.65. Then, the RE and MAPE values decreased significantly when the Brazilian test was performed on the rocks with a single magnitude of grain size. Moreover, BTS of fine-grained rocks are more reliable than coarse-grained rocks in UCS prediction. This can be certified by the narrower RE range (from -27.31 to 8.95%) and smaller MAPE value (11.01). Thus, the coarse grain size exerts a negative influence on the accuracy of estimated UCS.

Rock samples with $\beta = 90^\circ$ are the most reliable for estimating UCS, where the RE values range from 21.19 to 9.52% and the MAPE is 10.72 (see Fig. 9). Also, BTS of samples containing horizontal anisotropy show inferior reliability in the prediction of UCS, reflected by the wider RE range (from 22.97 to 38.54%) and higher MAPE value (18.52). For the rocks with three anisotropy inclinations (i.e. $\beta = 0^\circ, 45^\circ, 90^\circ$), the RE values fluctuate within a relatively wide range and change between 63.76% and 50.78%. When the rocks contain two anisotropy orientations (i.e. $\beta = 0^\circ, 45^\circ$), the estimated capability of BTS is enhanced slightly, where the MAPE declines from 26.44 to 23.42. Hence, the anisotropy inclination plays a major role in the UCS predictive performance of the Brazilian test.

Comparison study

Previous equations of UCS-BTS from sandstone and granite (no previous equations from gneiss) are used to predict UCS through the BTS data of this study. The comparisons between the measured UCS (black dots) and

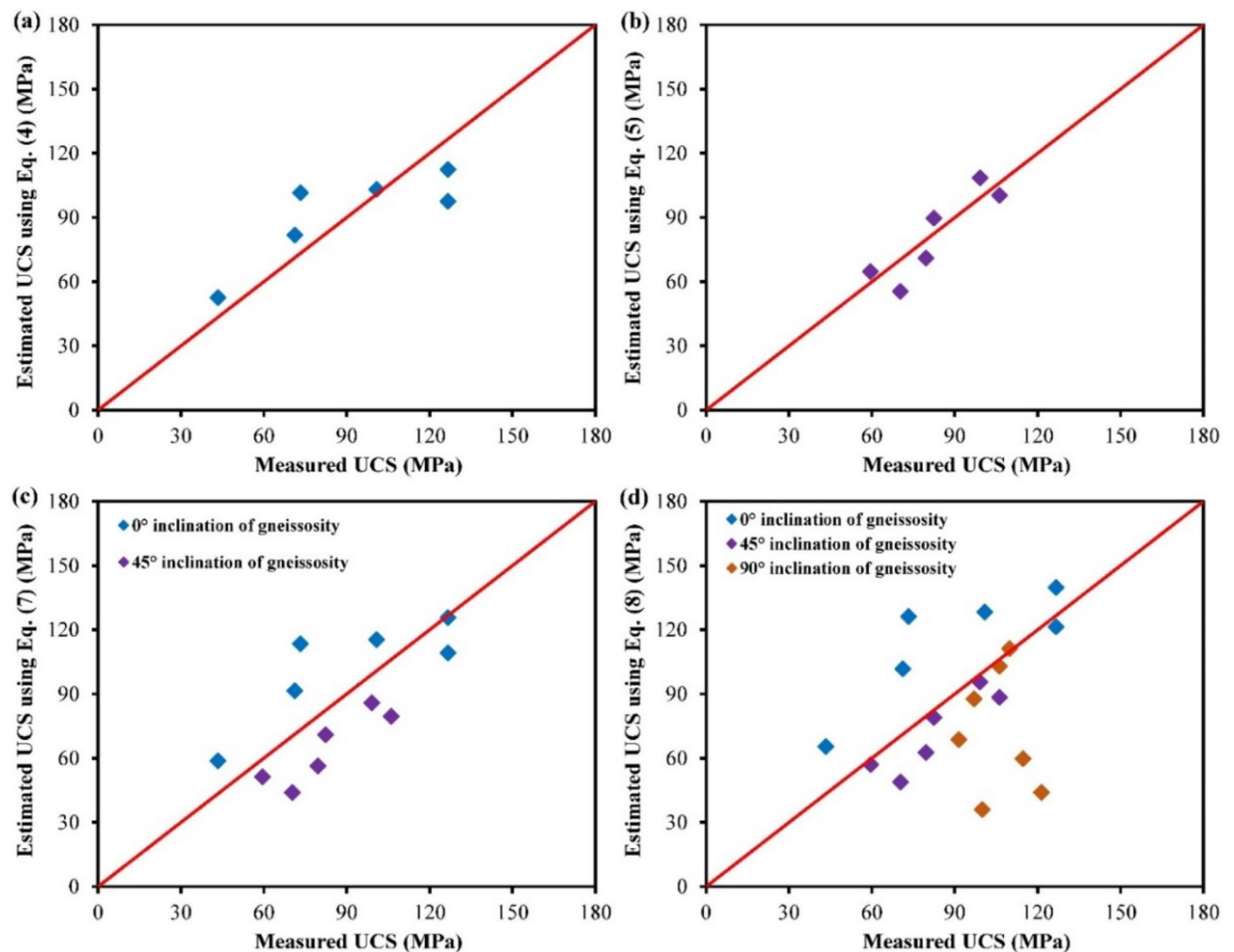


Fig. 7. Estimated capabilities of the derived equations of gneiss. (a) Samples with horizontal anisotropy; (b) samples with 45° inclined anisotropy; (c) samples with 45° and 90° inclined anisotropy; (d) all gneiss samples.

No.	Actual UCS (MPa)	Estimated UCS using Eq. (1)			Estimated UCS using Eq. (2)			Estimated UCS using Eq. (3)		
		Value (MPa)	RE (%)	MAPE	Value (MPa)	RE (%)	MAPE	Value (MPa)	RE (%)	MAPE
A	81.53	59.27	−27.31	11.04	–	–	–	71.61	−12.17	28.65
B	86.11	84.39	−2.00		–	–	–	101.96	18.40	
C	97.13	105.15	8.26		–	–	–	127.04	30.80	
D	85.88	93.57	8.95		–	–	–	113.05	31.63	
E	158.97	166.53	4.76		–	–	–	201.20	26.57	
F	112.35	111.47	−0.78		–	–	–	134.68	19.88	
G	81.71	61.07	−25.25		–	–	–	73.79	−9.69	
H	137.14	–	–	–	146.15	6.57	20.93	89.60	−34.66	
I	105.01	–	–	–	91.60	−12.77		56.16	−46.52	
J	116.15	–	–	–	107.61	−7.35		65.98	−43.20	
K	131.70	–	–	–	96.64	−26.62		59.25	−55.01	
L	57.37	–	–	–	73.82	28.67		45.26	−21.11	
M	114.44	–	–	–	101.68	−11.15		62.34	−45.53	
N	72.47	–	–	–	111.17	53.39		68.16	−5.96	

Table 5. The relative errors of estimated UCS based on derived equations for sandstone.

No.	Actual UCS (MPa)	Estimated UCS by Eq. (4)			Estimated UCS by Eq. (5)			Estimated UCS by Eq. (7)			Estimated UCS by Eq. (8)		
		Value (MPa)	RE (%)	MAPE	Value (MPa)	RE (%)	MAPE	Value (MPa)	RE (%)	MAPE	Value (MPa)	RE (%)	MAPE
A	71.20	81.75	14.83	18.52	–	–	–	91.43	28.42	23.42	101.70	42.85	26.44
B	126.67	97.57	– 22.97		–	–	–	109.12	– 13.86		121.38	– 4.18	
C	126.68	112.36	– 11.31		–	–	–	125.66	– 0.81		139.78	10.34	
D	100.80	103.12	2.30		–	–	–	115.32	14.40		128.28	27.26	
E	43.39	52.58	21.20		–	–	–	58.81	35.55		65.42	50.78	
F	73.25	101.47	38.54		–	–	–	113.48	54.93		126.24	72.35	
G	99.07	–	–	10.72	108.50	9.52	10.72	85.92	– 13.28	23.42	95.57	– 3.53	
H	59.53	–	–		64.69	8.68		51.23	– 13.94		56.99	– 4.27	
I	79.58	–	–		71.07	– 10.69		56.28	– 29.28		62.61	– 21.33	
J	106.13	–	–		100.37	– 5.42		79.48	– 25.11		88.42	– 16.69	
K	70.31	–	–		55.41	– 21.19		43.88	– 37.60		48.81	– 30.58	
L	82.38	–	–		89.64	8.81		70.98	– 13.84		78.96	– 4.15	
M	106.08	–	–	–	–	–	–	–	–	–	102.98	– 2.92	
N	99.89	–	–	–	–	–	–	–	–	–	36.03	– 63.93	
O	96.93	–	–	–	–	–	–	–	–	–	87.65	– 9.57	
P	121.30	–	–	–	–	–	–	–	–	–	43.95	– 63.76	
Q	109.85	–	–	–	–	–	–	–	–	–	111.16	1.19	
R	114.64	–	–	–	–	–	–	–	–	–	59.80	– 47.84	
S	91.37	–	–	–	–	–	–	–	–	–	68.74	– 24.77	

Table 6. The relative errors of estimated UCS based on derived equations for gneiss.

the estimated values are shown in Figs. 10 and 11. Each column represents an individual correlation, and the data points are estimated UCS values from the empirical equation.

As seen in Fig. 10, using improper empirical formulas can give rise to significant errors in estimated UCS, for example, the predicted UCS of 3.68 MPa from Hobbs (1967). The previous equations via sandstones have different grain-size characteristics, and this property results in considerable discrepancies between the actual and estimated UCS, where the maximum underestimation of UCS is 89.5%. Even though the sandstone samples used in this study, coarse grain leads to dramatic discrepancies in estimated UCS, the maximum overestimation of UCS reaches up to 44.0%.

Similarly, a very small estimated UCS value (3.44 MPa) can be seen from the equation proposed by Altindag and Guney (2010), and this evident error derives from the influences of different anisotropic properties (Fig. 11). Also, the discrepancies between actual and predicted UCS are noticeable, with a maximum underestimation of UCS of 90.7%. For the gneiss samples used in this study, the Brazilian test ignoring anisotropy inclination can generate errors of estimated UCS. However, this phenomenon is not significant, where the maximum overestimation of UCS is 3.7%.

Conclusion

In this study, the influence of grain size or anisotropy on the correlation of UCS-BTS is explored using sandstone (fine or coarse grain size) and gneiss (0°, 45°, 90° inclined anisotropy) samples. Based on the data of laboratory experiments, correlated relations between UCS and BTS are derived from via regression analysis. It is noted that several significant formulas for estimating UCS can be established with BTS, except for rocks with vertical anisotropy. The grain size variation or multidirectional anisotropy led to a decline in the *R*² value of correlations.

Also, the two other statistical parameters including AIC and PI, used to assess the UCS estimation performance, are compromised by grain size and anisotropy orientation. Coarse grain and multidirectional anisotropy can generate big AIC and small PI values. For rocks with fine grain size or unidirectional anisotropy, the data points of estimated UCS are clustered uniformly around the exact estimation line. The accuracy of estimated UCS can be improved when the Brazilian test is performed on a rock with a single magnitude of grain size or unidirectional anisotropy. The comparison study shows that using empirical formulas with different properties of grain size or anisotropy can generate significant errors in estimated UCS.

It is recommended that the Brazilian test be conducted separately on the fine- or coarse-grained rock. The coarse-grained rock must be with much care for predicting UCS via BTS. For highly anisotropic rock, BTS from rocks with unidirectional anisotropy is highly advisable when estimating UCS. However, the Brazilian test parallel to the anisotropy cannot be used to derive the correlation of UCS-BTS. The above findings can offer guidance for the Brazilian test to estimate UCS in the design of rock engineering, which can improve the accuracy of predicted UCS. However, this study only explored three anisotropy orientations and the critical inclination of anisotropy that leads to no significant correlation of UCS-BTS remains understood. The effects of other anisotropy inclinations on the correlation between UCS and BTS are expected to be investigated in future research.

Moreover, the proposed correlations can potentially be used to predict UCS through the Brazilian tensile strength on rocks with the same lithology, but with much care of grain size or anisotropy. Also, the emphasis of

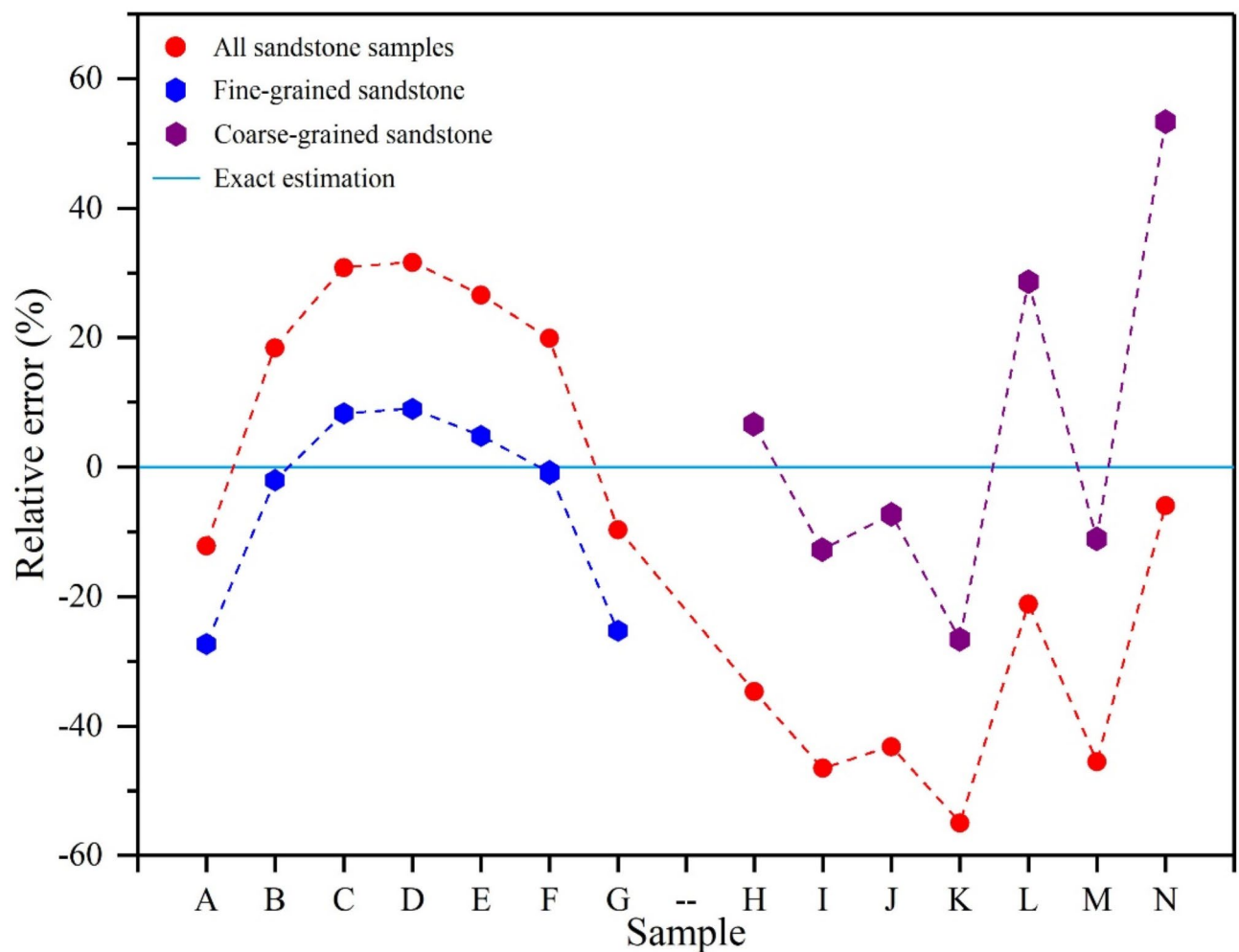


Fig. 8. The relative errors of estimated UCS using the proposed equations of sandstones.

this study was placed on the variable of grain size or anisotropy rather than the lithology. Hence, the applicability of this study can be extended to other heterogeneous rocks, such as limestone (with grain size variation) or shale (with anisotropy). Overall, the results can provide guidance for using the BTS to estimate UCS in evaluating the stability and service life of civil structures.

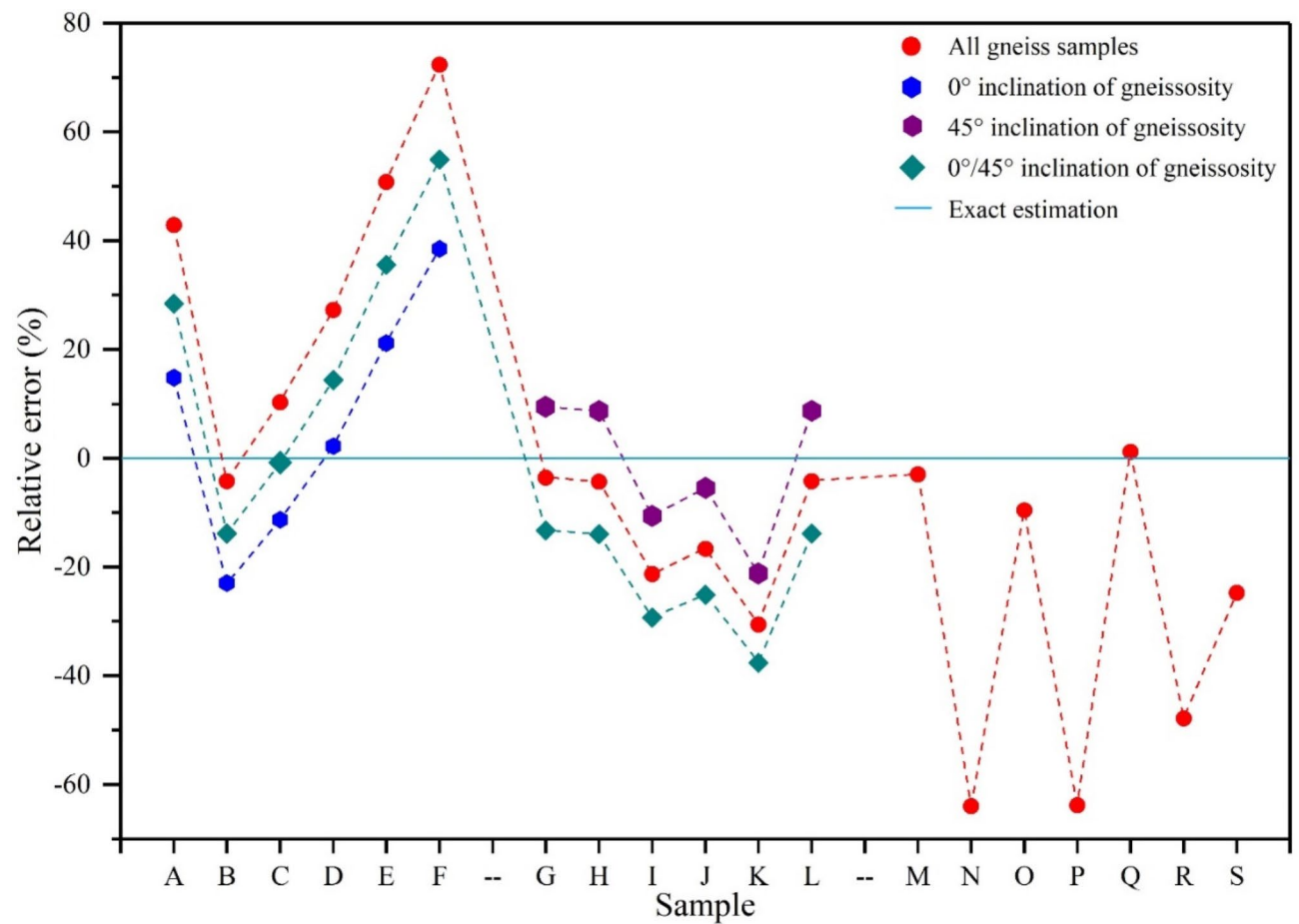


Fig. 9. The relative errors of estimated UCS using the proposed equations of gneisses.

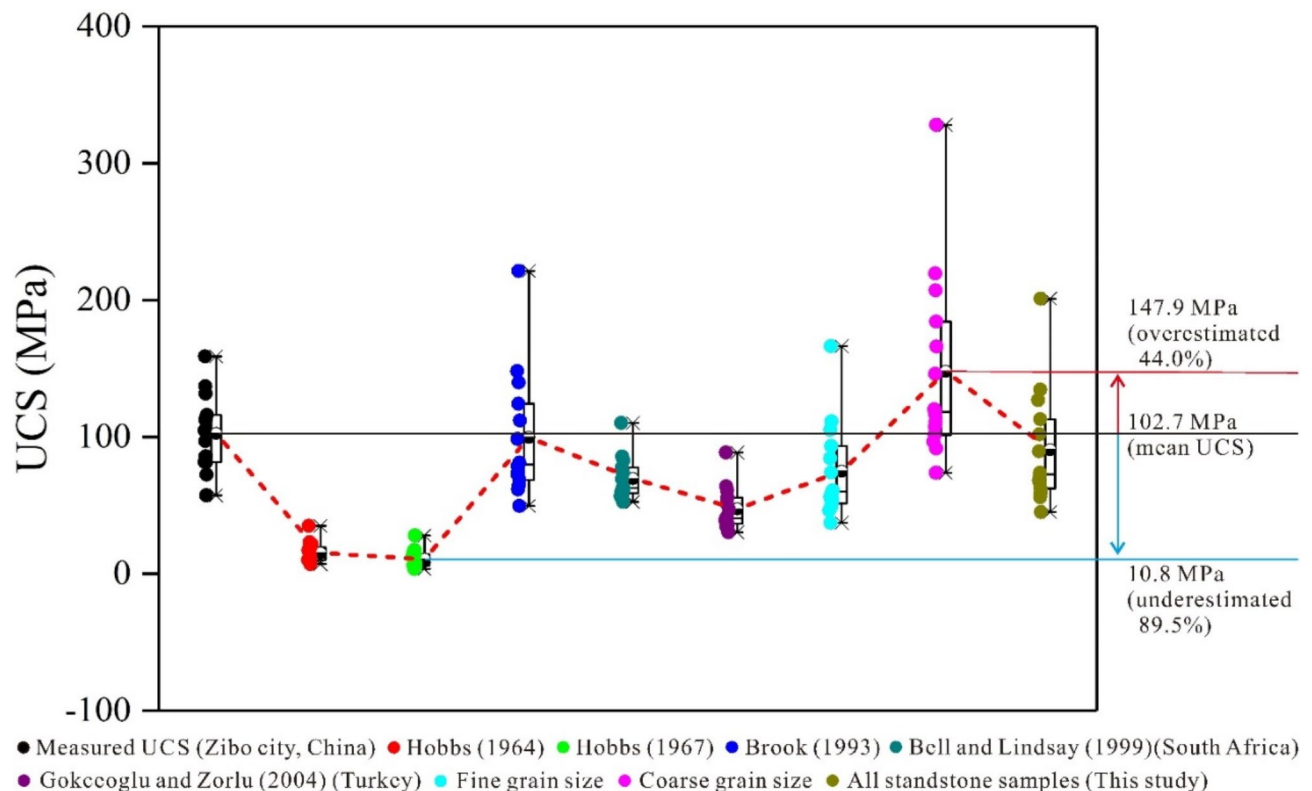


Fig. 10. Comparison between measured UCS and estimated UCS using previous formulas from sandstone.

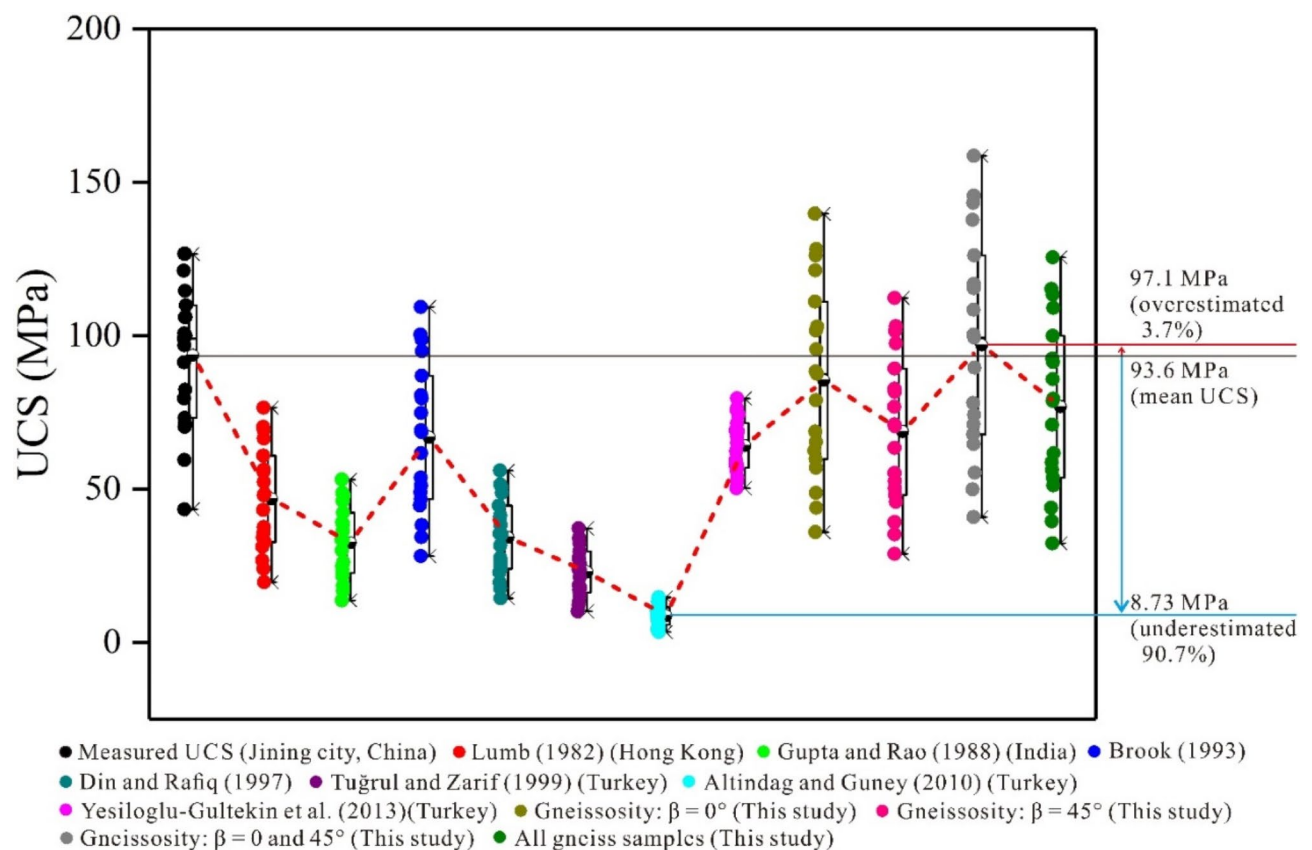


Fig. 11. Comparison between measured UCS and estimated UCS using previous formulas from granite.

Data availability

Data is provided within the Tables 2, and 3 of the manuscript.

Received: 5 August 2024; Accepted: 26 December 2024

Published online: 02 January 2025

References

1. Bieniawski, Z. T. The point-load test in geotechnical practice. *Eng. Geol.* **9**, 1–11 (1975).
2. Cai, M. Practical estimates of tensile strength and Hoek-Brown strength parameter M_i of brittle rocks. *Rock. Mech. Rock. Eng.* **43** (2), 167–184 (2010).
3. Davarpanah, S. M., Sharghi, M., Vászrhelyi, B. & Török, Á. Characterization of Hoek–Brown constant M_i of quasi-isotropic intact rock using rigidity index approach. *Acta Geotech.* **17** (3), 877–902 (2022).
4. Basu, A. & Kamran, M. Point load test on schistose rocks and its applicability in predicting uniaxial compressive strength. *Int. J. Rock. Mech. Min. Sci.* **47** (5), 823–828 (2010).
5. Yin, J., Wong, R. H. C., Chau, W. K. T., Laib, J. & Zhao, G. Point load strength index of granitic irregular lumps: size correction and correlation with uniaxial compressive strength. *Tunn. Undergr. Space Tech.* **70**, 388–399 (2017).
6. Kong, F. et al. The formation mechanism of dynamic water and mud inrush geohazard triggered by deep-buried tunnel crossing active fault: insights from the geomechanical model test. *Tunn. Undergr. Space Tech.* **142**, 105437 (2023).
7. Ng, I. T., Yuen, K. V. & Lau, C. H. Predictive model for uniaxial compressive strength for Grade III granitic rocks from Macao. *Eng. Geol.* **199**, 28–37 (2015).
8. Shalabi, F., Cording, E. J. & Al-Hattamleh, O. H. Estimation of rock engineering properties using hardness tests. *Eng. Geol.* **90**, 138–147 (2007).
9. Xue, Y. et al. Zhou, B. Water and mud inrush hazard in underground engineering: genesis, evolution and prevention. *Tunn. Undergr. Space Tech.* **114**, 103987 (2021).
10. Xue, Y. et al. China starts the world's hardest sky-high Road project: challenges and countermeasures for Sichuan-Tibet railway. *Innov.* **2** (2), 100105 (2021).
11. ISRM. Suggested methods for determining the Uniaxial Compressive Strength and Deformability of Rock materials, in: Ulusay R., Hudson J.A. (Eds.), *The Complete ISRM Suggested Methods for rock Characterization, Testing and Monitoring: 1974–2006*. ISRM Turkish National Group, Ankara, 130–134 (2007).
12. ASTM. *Standard test Method for Determination of the Point load Strength Index of rock and Application to rock Strength Classifications. D5731-08* (ASTM International, 2008).
13. Aliyu, M. M. et al. Assessing the uniaxial compressive strength of extremely hard cryptocrystalline flint. *Int. J. Rock. Mech. Min. Sci.* **113**, 310–321 (2019).
14. Diamantis, K., Gartzos, E. & Migiros, G. Study on uniaxial compressive strength, point load strength index, dynamic and physical properties of serpentinites from Central Greece: test results and empirical relations. *Eng. Geol.* **108**, 199–207 (2009).
15. Kong, F. M., Xue, Y. G., Qiu, D. H., Song, Q. & Chen, Q. Influence of grain size or anisotropy on the correlation between uniaxial compressive strength and sound velocity. *Bull. Eng. Geol. Environ.* **81**, 219 (2022).
16. Kong, F., Xue, Y., Qiu, D., Gong, H. & Ning, Z. Effect of grain size or anisotropy on the correlation between uniaxial compressive strength and Schmidt hammer test for building stones. *Constr. Build. Mater.* **299**, 123941 (2021).
17. Kong, F. M. & Shang, J. L. A validation study for the estimation of uniaxial compressive strength based on index tests. *Rock. Mech. Rock. Eng.* **51** (1), 2289–2297 (2021).
18. Xue, Y. G. et al. Using indirect testing methods to quickly acquire the rock strength and rock mass classification in tunnel engineering. *Int. J. Geomech.* **20** (5), 05020001 (2020).
19. Xue, Y. G., Kong, F. M., Qiu, D. H., Gong, H. & Ning, Z. Assessing the effect of grain size or anisotropy on the correlated equations between uniaxial compressive strength and point load test. *Bull. Eng. Geol. Environ.* **81** (8), 325 (2021).
20. Hosking, J. R. A comparison of tensile strength, crushing strength and elastic properties of roadmaking rocks. *Quarry Man. J.* **39**, 200–211 (1955).
21. Pomeroy, C. D. & Foote, P. A. Laboratory investigation of the relation between ploughability and the mechanical properties of coal. *Colliery Eng.* **37** (1), 146–154 (1960).
22. Szlavin, J. Relationships between some physical properties of rock determined by laboratory tests. *Int. J. Rock. Mech. Min. Sci. Geomech. Abstr.* **11** (2), 57–66 (1974).
23. Hobbs, D. W. The strength and the stress-strain characteristics of coal in triaxial compression. *J. Geol.* **72** (2), 214–231 (1964).
24. Hobbs, D. W. Rock tensile strength and its relationship to a number of alternative measures of rock strength. *Int. J. Rock. Mech. Min. Sci. Geomech. Abstr.* **4** (1), 115–127 (1967).
25. Lumb, P. Engineering properties of fresh and decomposed igneous rocks from Hong Kong. *Eng. Geol.* **19** (2), 81–94 (1983).
26. Gupta, A. S. & Rao, S. K. Index properties of weathered rocks: inter-relationships and applicability. *Bull. Eng. Geol. Environ.* **57** (2), 161–172 (1998).
27. Altindag, R. & Guney, A. Predicting the relationships between brittleness and mechanical properties (UCS, TS and SH) of rocks. *Sci. Res. Essays* **5** (16), 2107–2118 (2010).
28. Teme, S. C. An evaluation of the engineering properties of some Nigerian limestones as construction materials for highway pavements. *Eng. Geol.* **31** (3–4), 315–326 (1991).
29. Brook, N. New York, The measurement and estimation of basic rock strength (ed. Hudson, J.A.) (1993).
30. Lade, P. V. Rock strength criteria: the theories and the evidence (ed. Brown, E.T.) London, (1993).
31. Bell, F. G. & Lindsay, P. The petrographic and geomechanical properties of some sandstones from the Newspaper Member of the Natal Group near Durban, South Africa. *Eng. Geol.* **53** (1), 57–81 (1999).
32. Din, F. & Rafiq, M. Correlation between compressive strength and tensile strength/index strength of some rocks of North-West Frontier Province (limestone and granite). *Geol. Bull. Univ. Peshawar.* **30**, 183–190 (1997).
33. Tuğrul, A. & Zarif, I. H. Correlation of mineralogical and textural characteristics with engineering properties of selected granitic rocks from Turkey. *Eng. Geol.* **51** (4), 303–317 (1999).
34. Brady, B. H. G. & Brown, E. T. *Rock Mechanics for underground Mining* (New York, (2004).
35. Gokceoglu, C. & Zorlu, K. A fuzzy model to predict the uniaxial compressive strength and the modulus of elasticity of a problematic rock. *Eng. Appl. Artif. Intell.* **17** (1), 61–72 (2004).
36. Coviello, A., Lagioia, R. & Nova, R. On the measurement of the Tensile Strength of Soft Rocks. *Rock. Mech. Rock. Eng.* **38** (4), 251–273 (2005).
37. Arioglu, E. & Tokgoz, N. *Design and Essential of Hard Rock Mass & Coal Strength with Practical Solved Problems* Istanbul, (2011).
38. Kahraman, S. A. I. R., Fener, M. & Kozman, E. Predicting the compressive and tensile strength of rocks from indentation hardness index. *J. S Afr. I Min. Metall.* **112** (5), 331–339 (2012).
39. Rajabzadeh, M. A., Moosavinasab, Z. & Rakhshandehroo, G. Effects of Rock classes and porosity on the relation between Uniaxial Compressive Strength and some Rock properties for Carbonate Rocks. *Rock. Mech. Rock. Eng.* **45** (1), 113–122 (2012).
40. Sivakugan, N., Shukla, S. K. & Das, B. M. *Rock Mechanics: An Introduction* Boca Raton, (2013).

41. Yesiloglu-Gultekin, N., Gokceoglu, C. & Sezer, E. A. Prediction of uniaxial compressive strength of granitic rocks by various nonlinear tools and comparison of their performances. *Int. J. Rock. Mech. Min. Sci.* **62**, 113–122 (2013).
42. Karaman, K., Cihangir, F., Ercikdi, B., Kesimal, A. & Demirel, S. Utilization of the Brazilian test for estimating the uniaxial compressive strength and shear strength parameters. *J. S Afr. Ins Min. Metall.* **115** (3), 185–192 (2015).
43. Mohamad, E. T., Armaghani, D. J. & Momeni, E. Prediction of the unconfined compressive strength of soft rocks: a pso-based Ann approach. *Bull. Eng. Geol. Environ.* **74** (3), 745–757 (2015).
44. Fereidooni, D. Determination of the Geotechnical Characteristics of Hornfelsic Rocks with a Particular emphasis on the correlation between Physical and Mechanical properties. *Rock. Mech. Rock. Eng.* **49** (7), 2595–2608 (2016).
45. Ebdali, M., Khorasani, E. & Salehin, S. A comparative study of various hybrid neural networks and regression analysis to predict unconfined compressive strength of travertine. *Innov. Infrastruct. So.* **5** (3), 93–93 (2020).
46. Teymen, A. & Mengüç, E. C. Comparative evaluation of different statistical tools for the prediction of uniaxial compressive strength of rocks. *Int. J. Min. Sci. Tech.* **30** (6), 785–797 (2020).
47. Arman, H. Correlation of uniaxial compressive strength with indirect tensile strength (Brazilian) and 2nd cycle of slake durability index for evaporitic rocks. *Geotech. Geol. Eng.* **39** (2), 1583–1590 (2021).
48. Sadeghi, E., Nikudel, M. R., Khamchian, M. & Kavussi, A. Estimation of unconfined compressive strength (UCS) of Carbonate Rocks by Index Mechanical tests and specimen size properties: Central Alborz Zone of Iran. *Rock. Mech. Rock. Eng.* **55** (1), 125–145 (2022).
49. Kong, F. et al. Predicting uniaxial compressive strength of building stone based on index tests: correlations, validity, reliability, and unification. *Constr. Build. Mater.* **438**, 137227 (2024).
50. Jamshidi, A. & Torabi-Kaveh, M. Anisotropy in ultrasonic pulse velocity and dynamic elastic constants of laminated sandstone. *Q. J. Eng. Geol. Hydroge.* **54** (3), qjgh2020–qjgh2101 (2021).
51. Ajalloeian, R., Jamshidi, A. & Khorasani, R. Evaluating the effects of mineral grain size and mineralogical composition on the correlated equations between strength and Schmidt hardness of granitic rocks. *Geotech. Geol. Eng.* 1–11 (2020).
52. Tavallali, A. & Vervoort, A. Failure of layered sandstone under Brazilian test conditions: effect of micro-scale parameters on macro-scale behaviour. *Rock. Mech. Rock. Eng.* **43**, 641–653 (2010).
53. Kong, F. M. et al. Impact of grain size or anisotropy on correlations between rock tensile strength and some rock index properties. *Geomech. Eng.* **27** (2), 131–150 (2021).
54. Behrestaghi, M. H. N., Rao, K. S. & Ramamurthy, T. Engineering geological and geotechnical responses of schistose rocks from dam project areas in India. *Eng. Geol.* **44** (1–4), 183–201 (1996).
55. Jamshidi, A., Torabi-Kaveh, M. & Nikudel, M. R. Effect of anisotropy on the strength and brittleness indices of laminated sandstone. *IJST T Sci.* **45**, 927–936 (2021).
56. Kundu, J., Mahanta, B., Sarkar, K. & Singh, T. N. The effect of lineation on anisotropy in dry and saturated himalayan schistose rock under Brazilian test conditions. *Rock. Mech. Rock. Eng.* **51**, 5–21 (2018).
57. Zhang, S., Shou, K., Xian, X., Zhou, J. & Liu, G. Fractal characteristics and acoustic emission of anisotropic shale in Brazilian tests. *Tunn. Undergr. Space Technol.* **71**, 298–308 (2018).
58. China national standard. Standard for Test Methods of Engineering Rock Mass. Beijing, (2013).
59. Wang, M., Li, P., Wu, X. & Xu, D. Analysis of the stress ratio of anisotropic rocks in uniaxial tests. *Int. J. Min. Sci. Techno.* **27** (3), 531–535 (2017).
60. Khanlari, G. R., Heidari, M., Sepahi-Gero, A. A. & Fereidooni, D. Determination of geotechnical properties of anisotropic rocks using some index tests. *Geotech. Test. J.* **37** (2), 242–254 (2014).

Acknowledgements

Research in this paper is supported by the National Natural Science Foundation of China (grant numbers 42307228). The authors also express their thanks to the people helping with this work, and acknowledges the valuable suggestions from the peer reviewers.

Author contributions

Fanmeng Kong: Writing-Original draft preparation, Reviewing, Editing, Conceptualization, Methodology. Mingyi Han: Writing-Original draft preparation. Yuting Zhao: Conceptualization, Methodology. Haitao Lu: Reviewing, Editing. Shian Liu: Reviewing, Editing. Pengyu Luan: Reviewing, Editing. Baolong Zhuo: Reviewing, Editing. Gaofei Shi: Reviewing, Editing.

Declarations

Competing interests

The authors declare no competing interests.

Additional information

Correspondence and requests for materials should be addressed to F.M.K. or Y.T.Z.

Reprints and permissions information is available at www.nature.com/reprints.

Publisher's note Springer Nature remains neutral with regard to jurisdictional claims in published maps and institutional affiliations.

Open Access This article is licensed under a Creative Commons Attribution-NonCommercial-NoDerivatives 4.0 International License, which permits any non-commercial use, sharing, distribution and reproduction in any medium or format, as long as you give appropriate credit to the original author(s) and the source, provide a link to the Creative Commons licence, and indicate if you modified the licensed material. You do not have permission under this licence to share adapted material derived from this article or parts of it. The images or other third party material in this article are included in the article's Creative Commons licence, unless indicated otherwise in a credit line to the material. If material is not included in the article's Creative Commons licence and your intended use is not permitted by statutory regulation or exceeds the permitted use, you will need to obtain permission directly from the copyright holder. To view a copy of this licence, visit <http://creativecommons.org/licenses/by-nc-nd/4.0/>.

© The Author(s) 2024